nature nanotechnology

SUPPLEMENTARY INFORMATION

DOI: 10.1038/NNANO.2015.324

A transparent bending-insensitive pressure sensor

Sungwon Lee[1,2], Amir Reuveny[1,2], Jonathan Reeder[1#], Sunghoon Lee[1,2], Hanbit Jin[1,2], Qihan Liu[5], Tomoyuki Yokota[1,2], Tsuyoshi Sekitani[1,2,3], Takashi Isoyama[4], Yusuke Abe[4], Zhigang Suo[5] and Takao Someya[1,2]*

**Correspondence should be sent to Takao Someya (E-mail: someya@ee.t.u-tokyo.ac.jp).*

Keywords: Pressure sensor, Nano fiber, E-skin, Flexible electronics, Bending insensitivity.

DOI: 10.1038/NNANO.2015.324

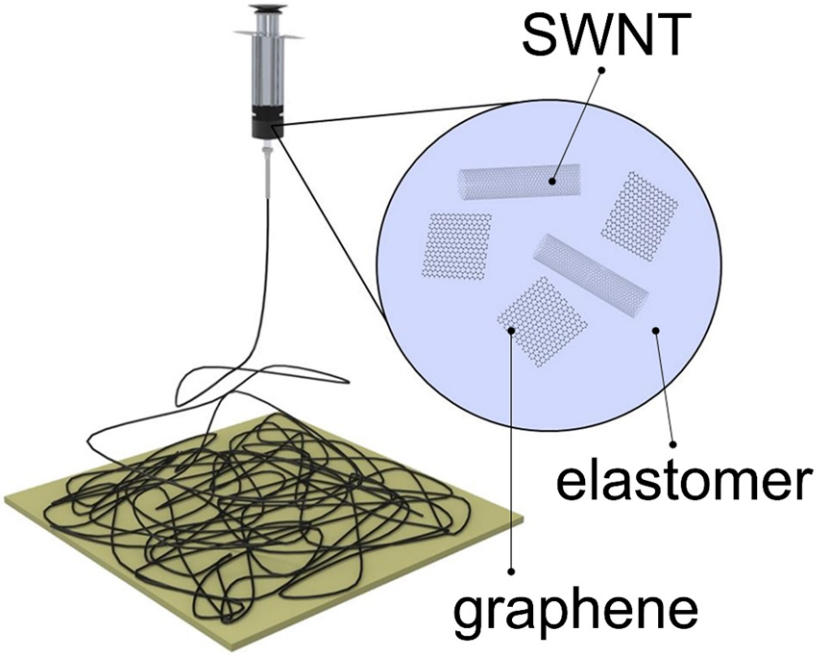

Supplementary Figure 1. **Electrospun pressure-sensitive nanofiber.** Schematic illustration of the fabrication of a pressure-sensitive nanofiber using the electrospinning process. The prepared solution is composed of elastomer (fluorinated copolymer, vinylidenefluoride-tetrafluoroethylene-hexafluoropropylene), CNT, graphene, and 4-methly-2-pentanone.

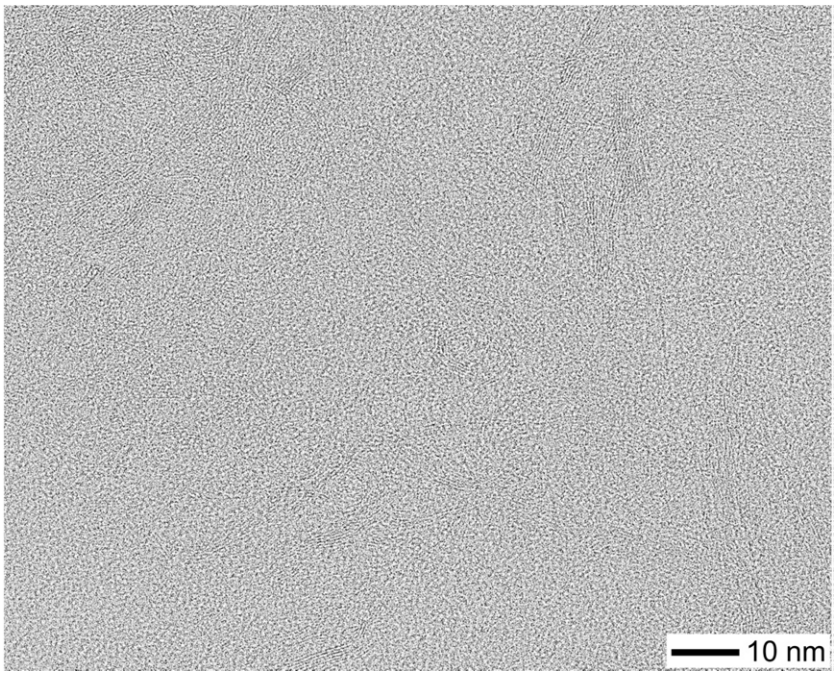

Supplementary Figure 2. **Electrospun pressure-sensitive nanofiber.** HRTEM image showing CNTs well dispersed in elastomer matrix.

DOI: 10.1038/NNANO.2015.324

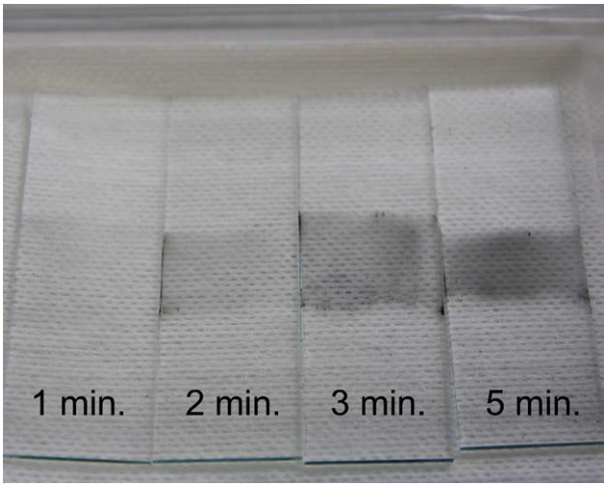

Supplementary Figure 3. **Influence of fiber-deposition time on transparency and pressure sensitivity.** Photograph of electrospun pressure-sensitive nanofiber on glass with different deposition times. The two-dimensional areal densities of the fibers are 15, 24, 33, and 48%, respectively.

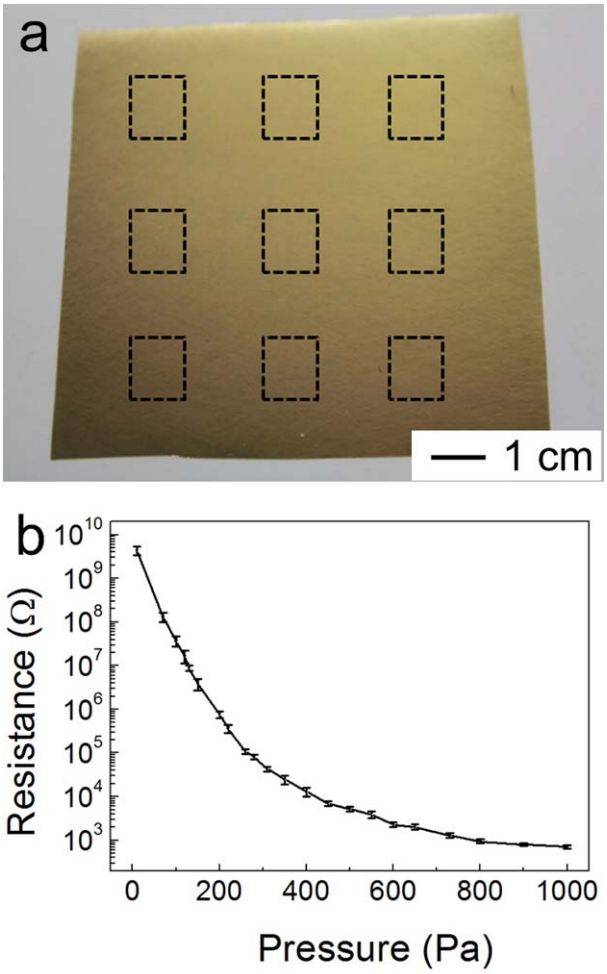

Supplementary Figure 4. **Areal uniformity of large sensor sheet. a**, Electrospun fiber on Au film (9 × 9 cm; the dashed line represents the measured area) for uniformity tests, and **b** average pressure response and standard deviation of the nine areas specified. The large-area uniformity of the electrospun fiber mesh was examined by depositing 9 × 9 cm^2 samples on Au-coated PET films. The top Au electrodes (1 cm^2) were deposited on another PET substrate, and pressure was applied at different locations on the large film.

DOI: 10.1038/NNANO.2015.324

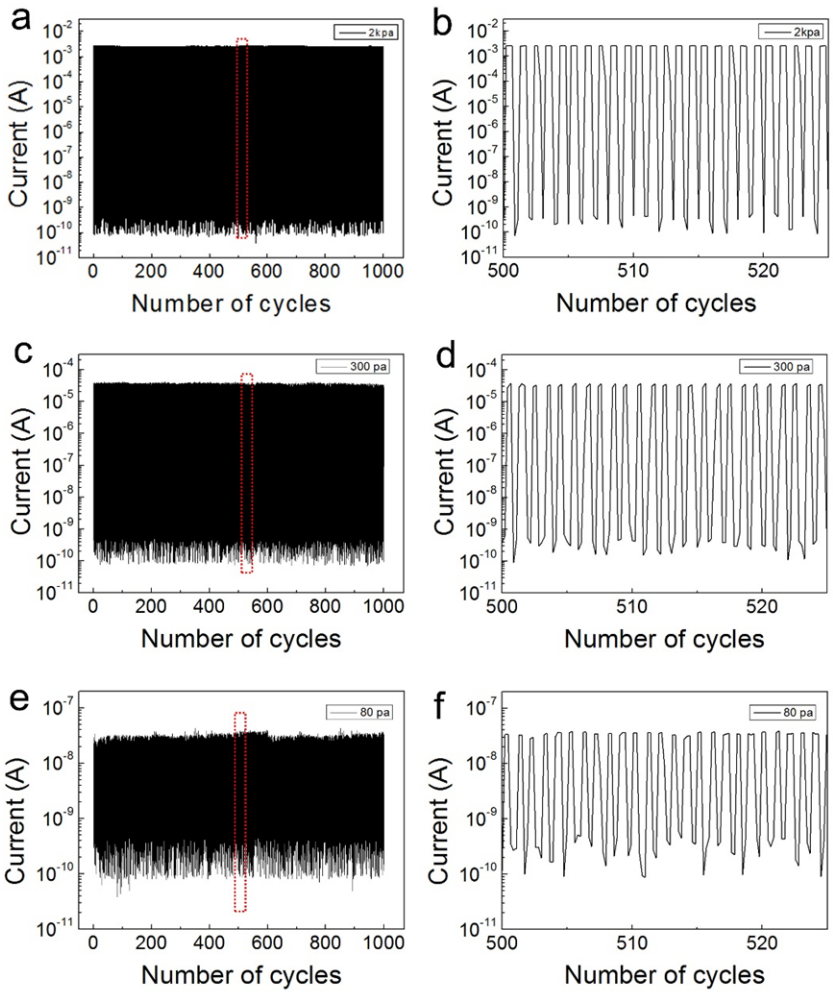

Supplementary Figure 5. **Reversibility of nanofiber pressure sensor.** Cyclic test of pressure sensor over 1000 cycles at 2 kPa (**a**, **b**), 300 Pa (**c**, **d**), and 80 Pa (**e**, **f**) using the same device.

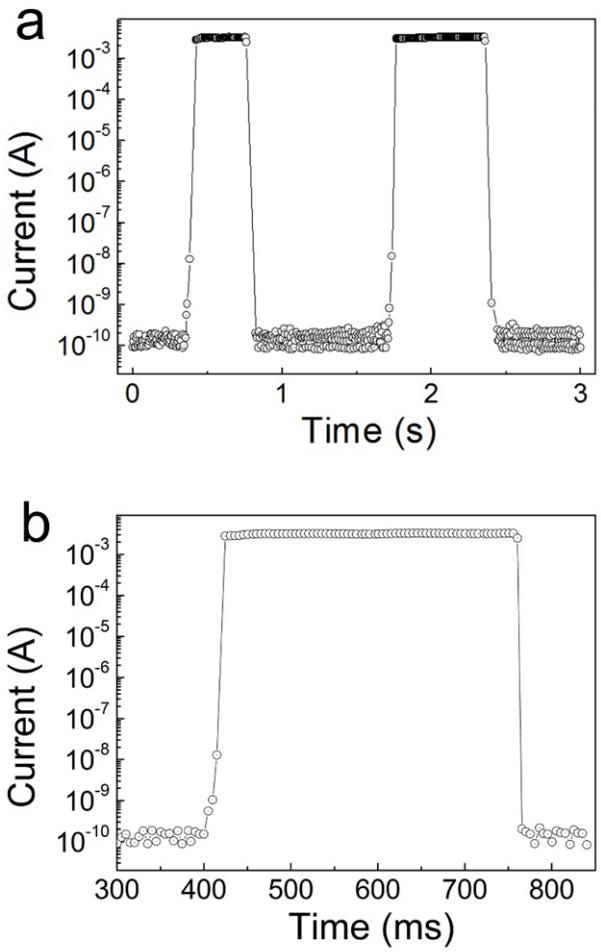

Supplementary Figure 6. **Response time of nanofiber pressure sensor.** Pressure response of sensor with measurement interval of 5 ms. **a**, Response measured for 3 s by pressing twice with finger. **b**, Pressure response to first pressing. We expect that the reason for the fast response time after releasing is due to the conduction mechanism. When pressure is applied, the fibers begin to make contact with each other, forming new electrical paths. Then, the fibers are compressed, which increases the conductivity itself. While being releases, concentrated compressive stress immediately repels the fibers from each other, increasing the decrease in the conductivity.

DOI: 10.1038/NNANO.2015.324

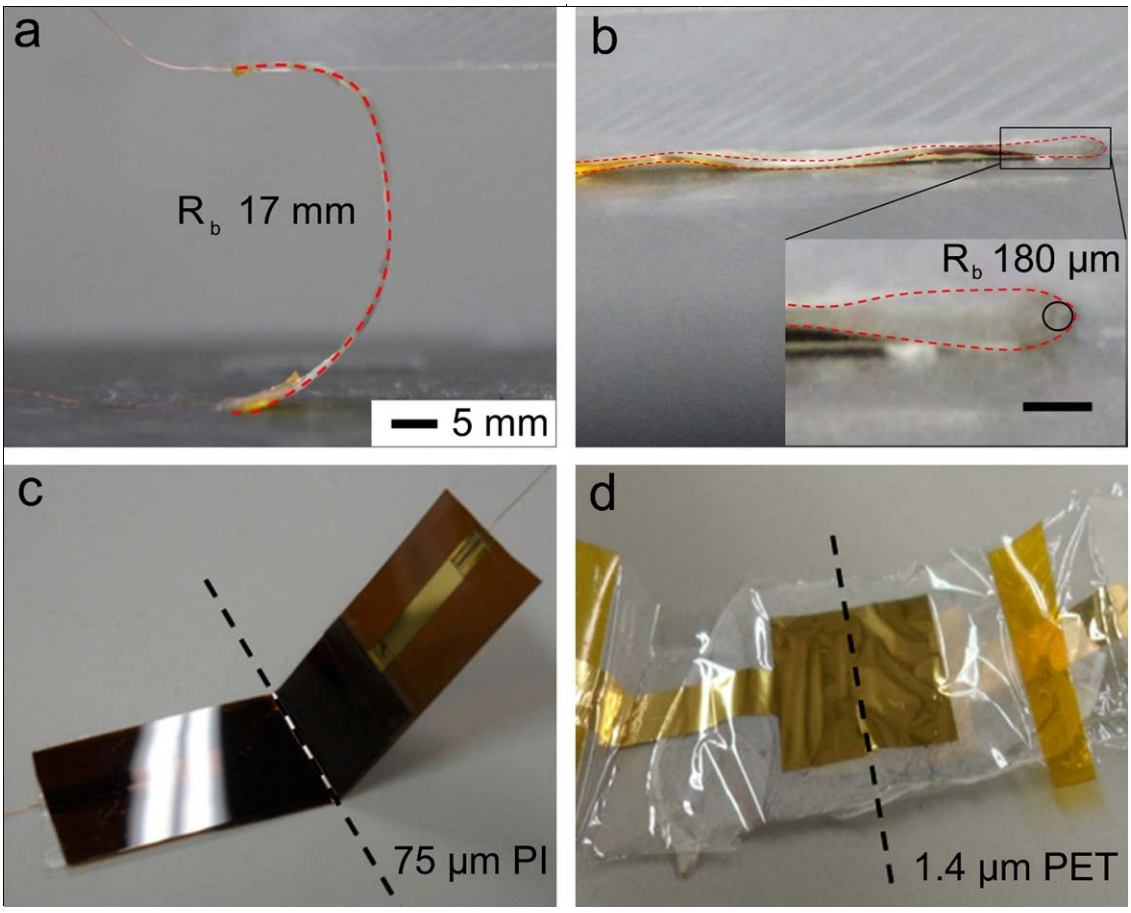

Supplementary Figure 7. **Robustness of device under bending. a**, Photograph of the device fabricated on 12.5-μm-thick PI substrate with a bending radius of 17 mm (red dashed line represents the device viewed from the side). **b**, Photograph of the device fabricated on 12.5-μm-thick PI substrate with a bending radius of 180 μm (red dashed line represents the device viewed from the side, scale bar represents 1 mm). **c**, Device fabricated on 75-μm-thick PI film after bending test. **d**, Device fabricated on 1.4-μm-thick PET after bending test. The black dashed line represents the fold line during the test.

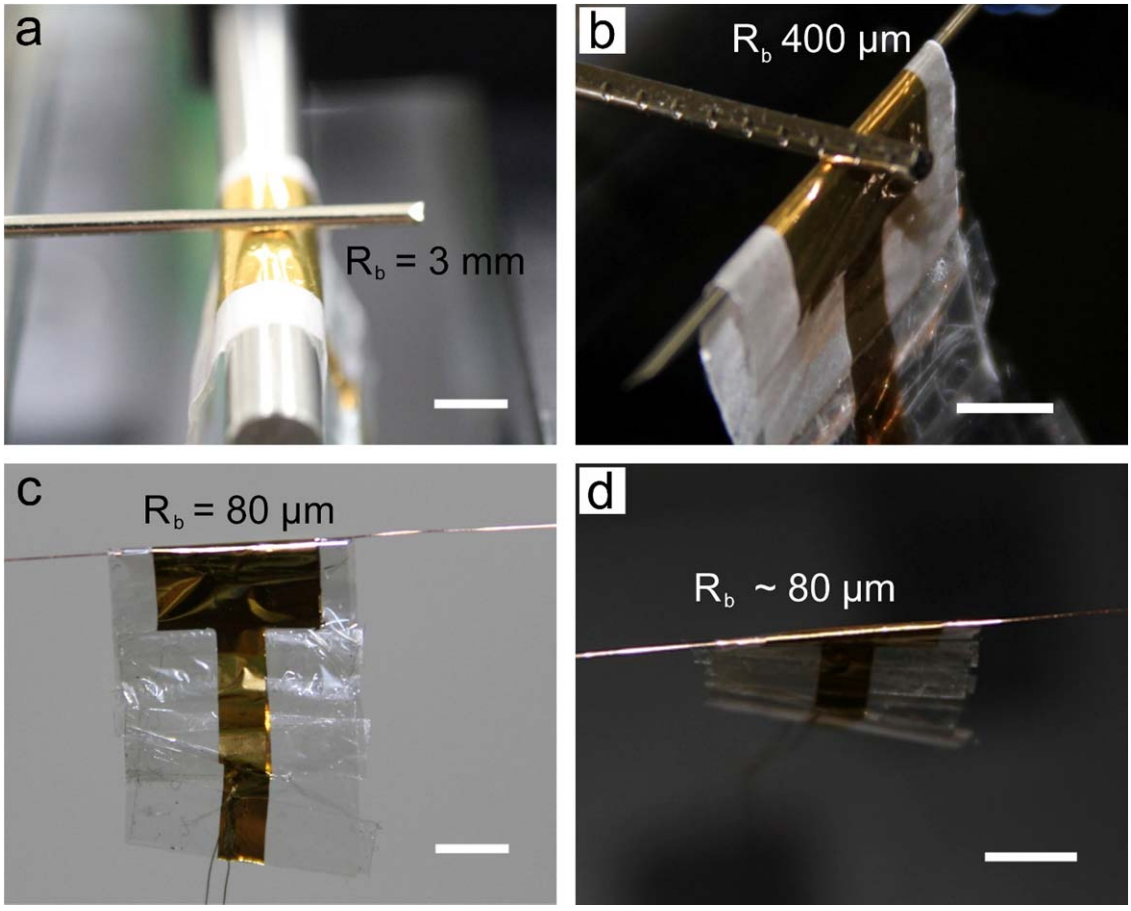

Supplementary Figure 8. **Pressure-response test in bent state. a**, Photograph showing the measurement of the sensor response for a bending radius of 3 mm. **b**, Photograph of the sensor under a bending radius of 400 µm for the measurement of the pressure response. Bending radii of 80 µm, **c** (front view), and top view, **d** (scale bars are 5 mm).

DOI: 10.1038/NNANO.2015.324

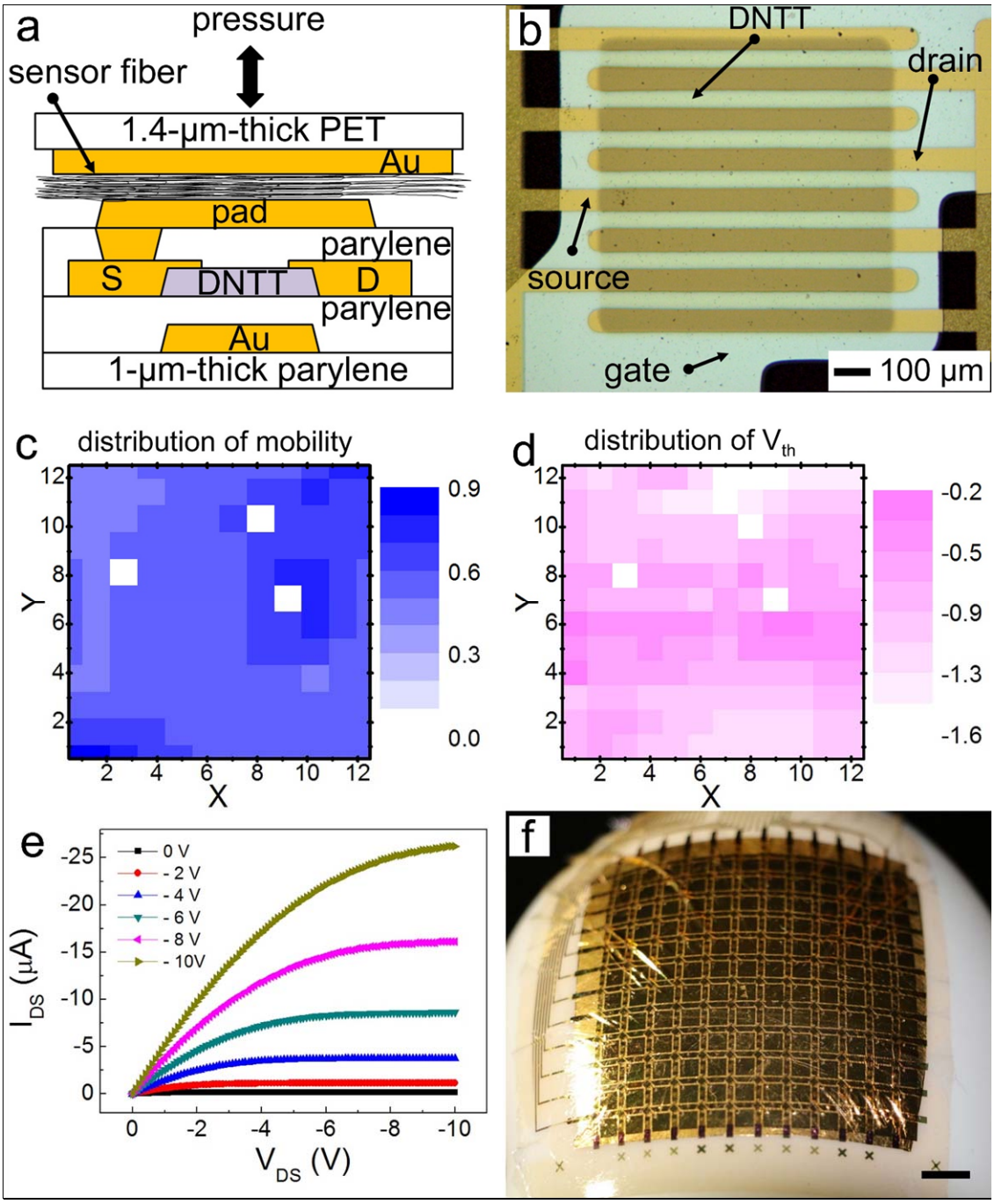

Supplementary Figure 9. **Integrated device. a**, Schematic illustration of vertical structure of single pressure sensor pixel. **b**, Micrograph of a single organic transistor (W/L = 100). **c**, Distribution of

mobility values of transistors in 144 pixels. **d**, Threshold voltage distribution of active matrix. **e**, Typical output characteristics of a transistor. **f**, Photograph of integrated sensor array attached to the surface of a soft balloon. (Scale bar represents 1 cm). The mobility of the transistors in the saturation regime was 0.5 ± 0.07 cm^2/Vs, the on/off ratio exceeded 10^4, and the threshold voltage was −0.8 ± 0.26 V with a yield of 97.9%.

DOI: 10.1038/NNANO.2015.324

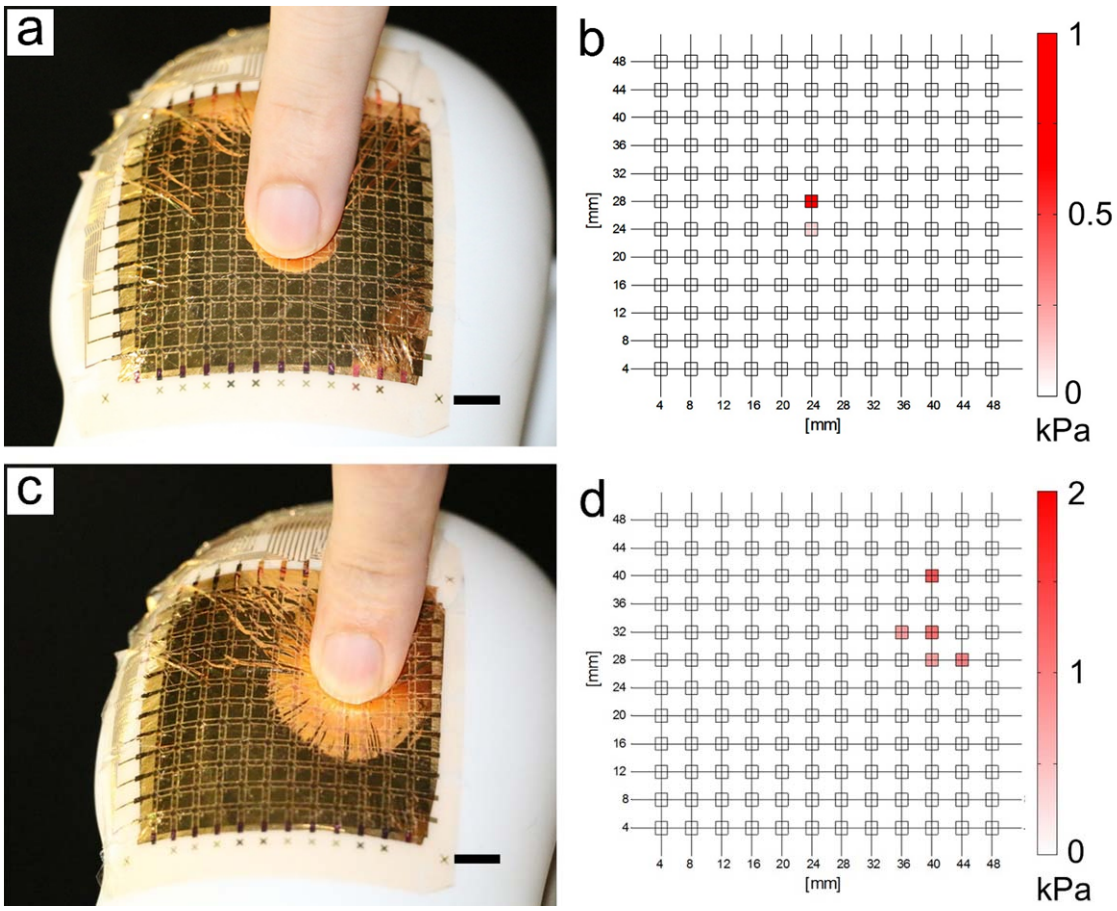

Supplementary Figure 10. **Pressure mapping of integrated device.** Photograph showing the slight touching of the center area **a**, and its pressure distribution data **b**, Photograph showing pressing of top right side **c**, and its pressure distribution data **d** (scale bars represent 1 cm).

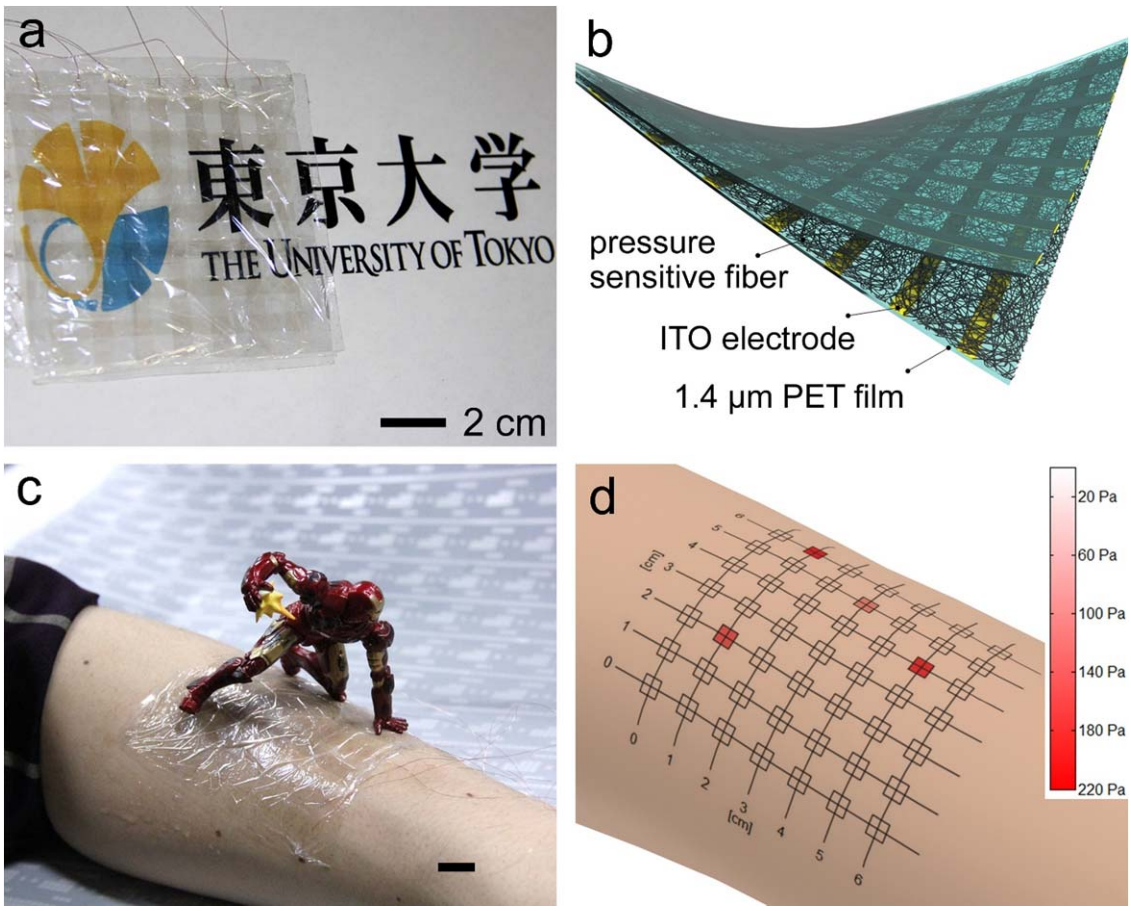

Supplementary Figure 11. **Transparent E-skin. a**, Photograph of transparent pressure-sensor array and its schematic illustration **b**. **c**, Images of sensor attached to arm and plastic model on top of it (scale bar represents 1 cm). **d**, Pressure distribution data from plastic model.

The nanofibrous sensors were fabricated in a transparent 7×7 matrix that has a large area (9×9 cm^2) and is both ultra-flexible and lightweight. The size of each cell was 5×5 mm^2, the spacing was 10 mm, and the total thickness was approximately 5 μm. Indium tin oxide (ITO) layers were deposited on the PET layer as transparent electrodes (Supplementary Figs. S8a and S8b). The sensor matrix was placed on a human arm and had good mechanical contact with the skin. A plastic object weighing 7 g was gently placed on the device; then, the resistance of each cell was measured. The pressure was measured only in

DOI: 10.1038/NNANO.2015.324

the areas making contact. No pressure was measured in the other areas although the device was bent (bending radius of roughly 5 cm) and highly wrinkled, thus demonstrating the feasibility of a highly sensitive, conformable, and bending-insensitive pressure sensor.

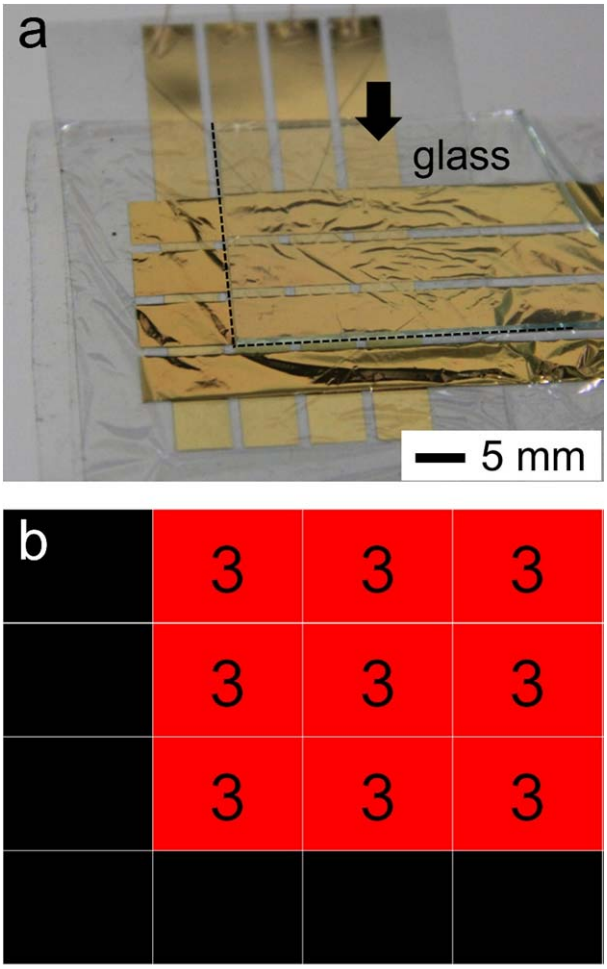

Supplementary Figure 12. **Testing interference of electrical signal. a**, Photograph of passive matrix sensor array with glass on top (the dashed line is the border of the glass). **b**, Measured pressure response while applying strong pressure on the glass. The maximum pressure that this device can detect is 3 kPa. The distance between pixels was 1 mm, and the unit is kPa.

We evaluated the crosstalk of the nanofiber layer using a 4×4 array of 1-mm^2 pixels with a 2-mm pitch. Strong pressure (>1 MPa) was selectively applied to certain pixels, and the pressure distribution was measured. An extremely small current (<100 pA at an applied voltage of 1 V) was measured at the pixels without pressure, showing that the device detects pressure reliably and accurately with a 1-mm spacing between pixels.

DOI: 10.1038/NNANO.2015.324

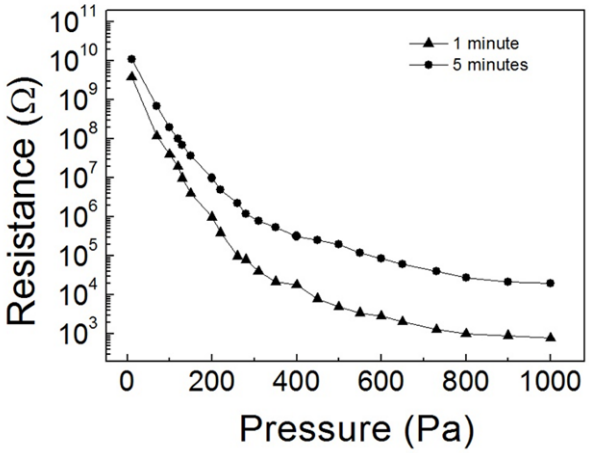

Supplementary Figure 13. **Pressure response of sensor with different deposition times.** A longer deposition time results in a less sensitive pressure sensor.

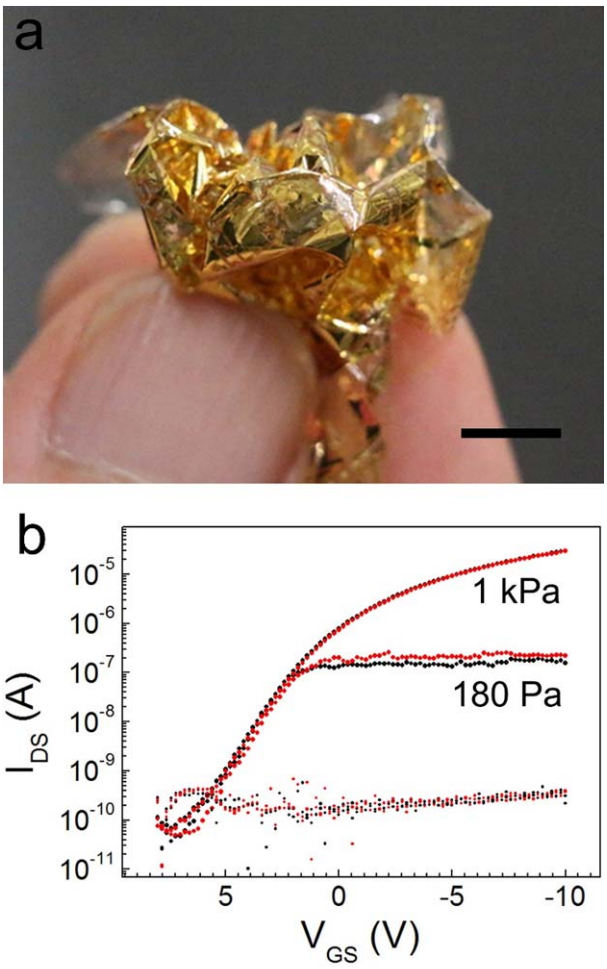

Supplementary Figure 14. **Mechanical robustness of a device. a**, A photograph of an integrated device that is crumpled (scale bar represents 1 cm). **b**, Pressure response (transfer curve) of one pixel before and after being crumpled 10 times (black represents before and red represents after).

DOI: 10.1038/NNANO.2015.324

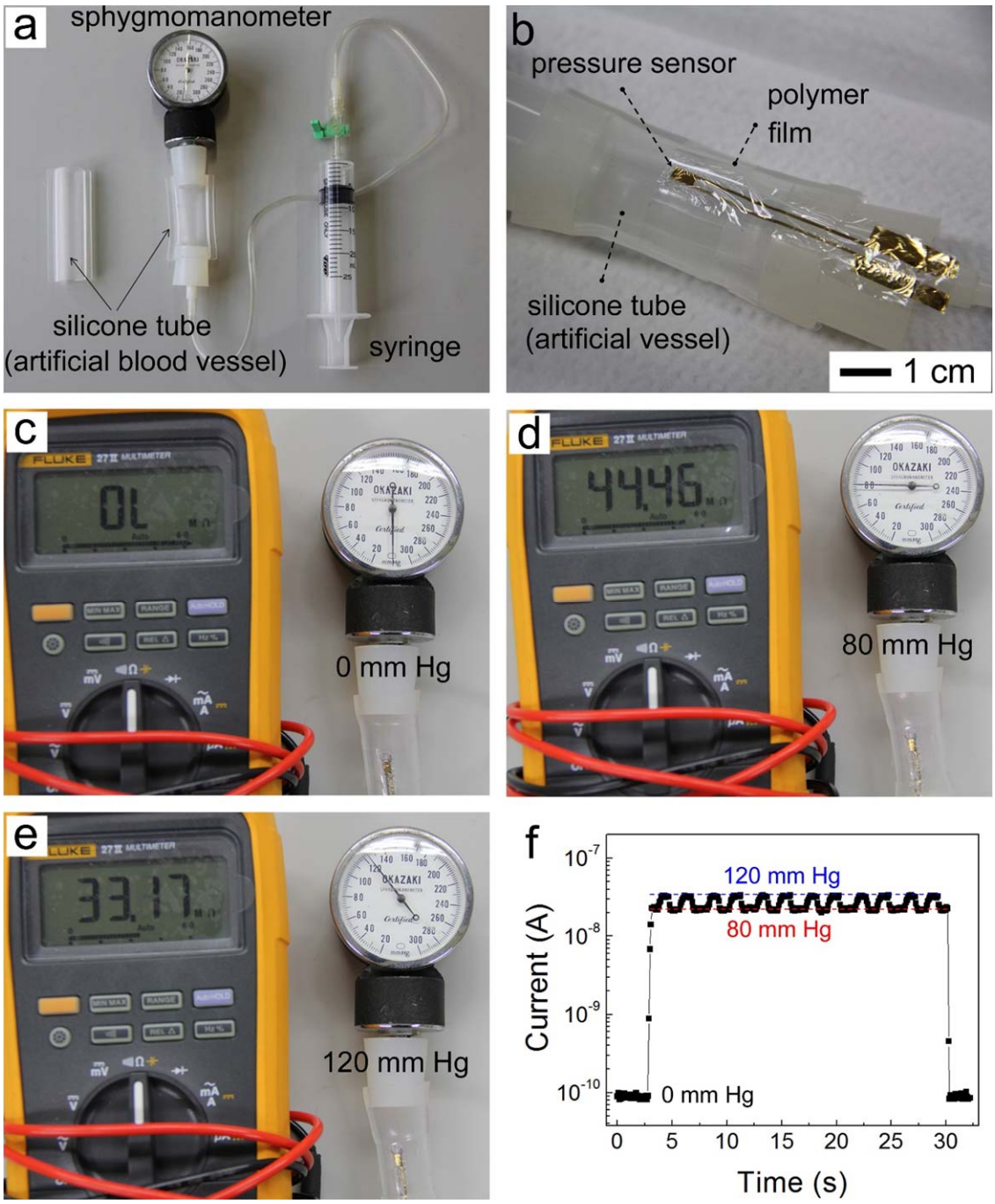

Supplementary Figure 15. **Pressure measurement from artificial blood vessel. a**, Photograph of measurement setup. **b**, Photograph of pressure sensor (sensor size is 2 mm × 4 mm, Supplementary

Movie 4) on artificial blood vessel. Measured resistance of sensor from artificial blood vessel model with **c** 0, **d** 80, and **e** 120 mm Hg. **f**, Measured current during the repeated pumping of air into the tube at an applied voltage of 1 V. A small pressure sensor was attached to the tube with an outer radius of 1 cm, and was wrapped by a polymer film to detect the expansion of the vessel. For preliminary testing, the model blood vessel was connected to an air-pressure sensor to monitor and control the pressure inside the tube.

DOI: 10.1038/NNANO.2015.324

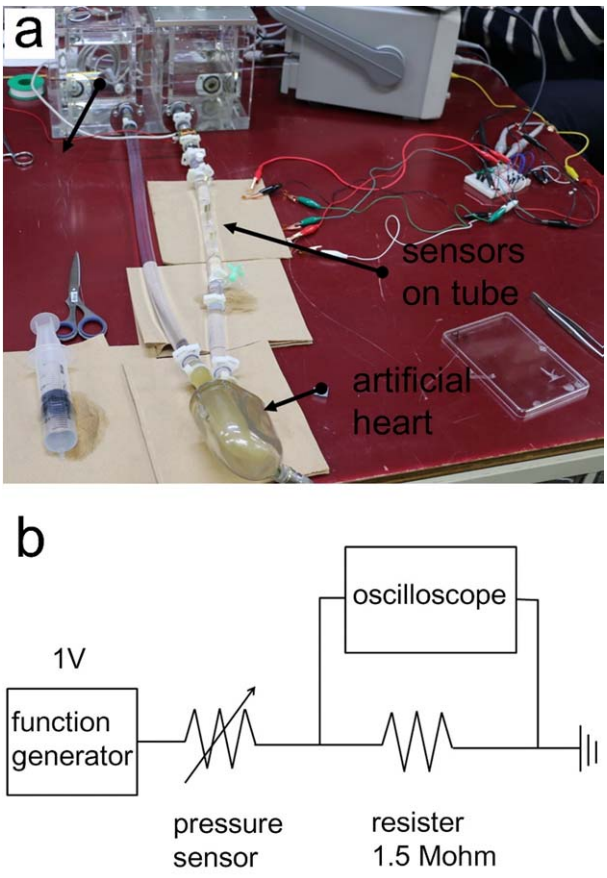

Supplementary Figure 16. **Experimental setup for measurement of pressure propagation from artificial blood vessel using artificial heart. a**, Photograph of measurement setup. **b**, Circuit diagram for the voltage measurement. Water pressure was applied using a displacement-type artificial heart system. The applied pressure was sufficiently high enough that it saturated the voltage (<10 kΩ at the sensor, which corresponds to >400 Pa) in this circuit.

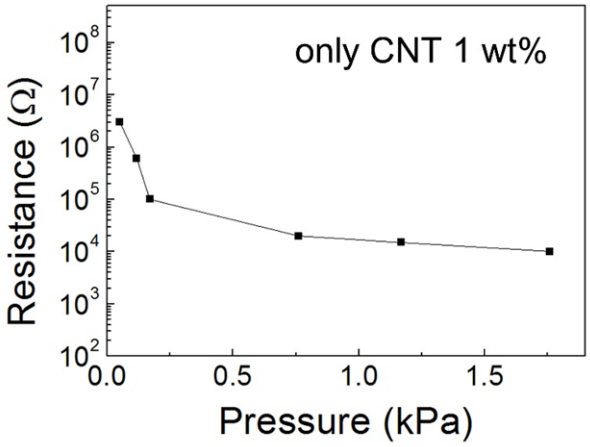

Supplementary Figure 17. **Pressure response of sensor without using graphene.** Sensitivity of the pressure-sensor device is much lower than that achieved using majority of graphene and small amount of CNTs.

DOI: 10.1038/NNANO.2015.324

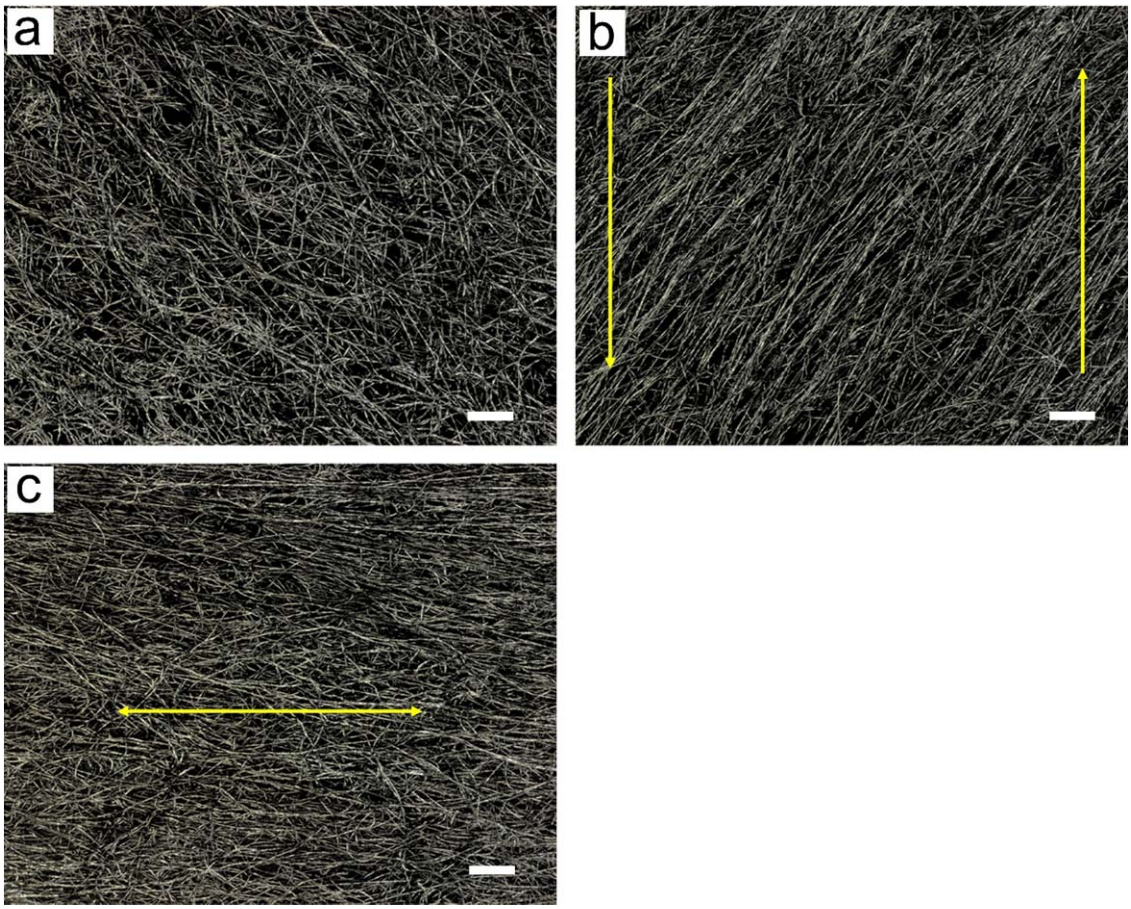

Supplementary Figure 18. **Nanofiber feature under strain.** Microscope images of **a**, as spun fiber layer, **b**, under large shear strain (40 %), and **c**, tensile strain (30 %) (Scale bars represent 20 μm). The nanofibers change their alignment to reduce the strain due to tensile stress.

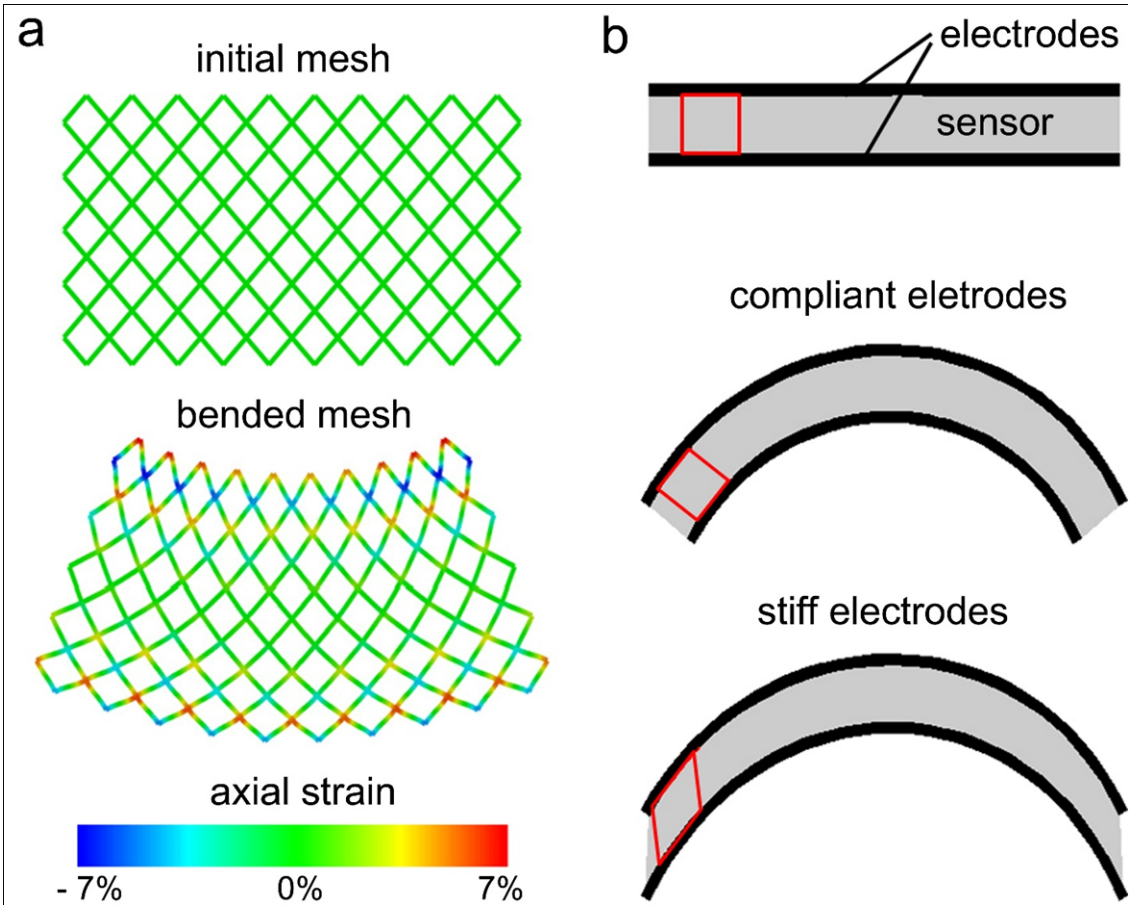

Supplementary Figure 19. **Numerical analysis of the bending of a fibrous mesh. a**, We study the bending sensitivity of a fibrous sheet. As a qualitative illustration, the fibrous material is represented by a square lattice of ligaments. The fibers are assumed to be bonded and not allowed to slide with respect to each other. The simulation is done using the commercial software ABAQUS, and individual fibers are represented using linear beam elements (B21). The fibers are modeled as a linear elastic material; the thickness-to-length ratio of each ligament is 1:7. The axial strain in the fibers is mapped with color. **b**, In real device structure, the fibrous sensor layer is sandwiched between two electrodes. When the electrodes are compliant, the sensor layer bends freely. The top electrode is compressed and the

DOI: 10.1038/NNANO.2015.324

bottom electrode is stretched. When the electrodes are stiff, however, each electrode bends freely but does not stretch or compress, so that the sensor layer is sheared. The shear strain is maximum at the edge of the sandwiched structure and the shear strain is larger if the sandwiched structure is longer. This phenomenon is one of the reasons for which devices with a thinner electrode and sensing layer have less strain, thus diminishing the electrical properties when devices are bent.

Movie S1. A movie showing the uniformity of a large-area pressure response. The size of the device is 9 cm × 9 cm with a pressure-sensitive nanofiber layer deposited uniformly on the bottom Au film. Then, a 1 cm^2-sized top electrode is pressing a different area.

Movie S2. A movie showing the pressure response of the sensor under a completely folded state. The center of the device was folded on thin Cu wire. The bending radius of the sensor was approximately 80 μm.

Movie S3. A movie showing the pressure response of an integrated sensor attached to a soft balloon, and showing the distribution of the pressure under complex deformation.

Movie S4. A movie showing the pressure response of a sensor attached to a fingertip and pressed by another finger. The bending radius of the finger was approximately 7 mm.